

We are IntechOpen, the world's leading publisher of Open Access books Built by scientists, for scientists

6,900

Open access books available

185,000

International authors and editors

200M

Downloads

Our authors are among the

154

Countries delivered to

TOP 1%

most cited scientists

12.2%

Contributors from top 500 universities



WEB OF SCIENCE™

Selection of our books indexed in the Book Citation Index
in Web of Science™ Core Collection (BKCI)

Interested in publishing with us?
Contact book.department@intechopen.com

Numbers displayed above are based on latest data collected.
For more information visit www.intechopen.com



Influence of Tribological Parameters on the Railway Wheel Derailment

*George Tumanishvili, Tengiz Nadiradze
and Giorgi Tumanishvili*

Abstract

At present, Nadal's formula is used for prediction of derailment that contains a limited number of parameters. Besides, insufficient study of laws of variation of the noted parameters and ignorance of the influence of other parameters on the derailment complicate solution of the problem. The sliding distance and the relative sliding velocity are the most sensitive factors contributing to the destruction of the third body. Moreover, increased friction coefficient between the steering surfaces of the wheel and rail promotes climbing of a wheel on the rail and derailment. Dependences of the main parameters, influencing the destruction of the third body, the sliding distance and the relative sliding velocity on the rail track curvature, and difference of diameters of wheels of the wheelset and the non-roundness of one of the wheels of the wheelset are shown in the work. The methods for estimation of the third body destruction degree and consideration in Nadal's formula of the additional criterion of impossibility of the wheel rolling on the contact point of the wheel and rail steering surfaces, containing a value of this contact point advancing, which in turn depends on the angle of attack, are proposed.

Keywords: tribological parameters, derailment, sliding distance, wear rate, third body

1. Introduction

The correlation of lateral and vertical forces, angle of inclination of the wheel flange, and coefficient of friction between the wheel flange and rail gauge are considered as main parameters acting on derailment [1]. Avoidance of derailment and ensuring durability of the wheelsets, rails, brake shoes, etc. are vital for railways for both safety and economic reasons [2]. The prevalent case of derailments is climbing of a wheel on the rail that is influenced by such main parameters as the flange angle, vertical and lateral forces, angle of attack, friction factors, etc. There are many works devoted to these phenomena [1, 3–13] that indicate urgency of the problem.

The climbing of the wheel on the rail is stipulated by the tribological, geometric, and dynamical parameters of the wheel-rail interaction. For the solution of the problem, qualitative and quantitative estimations of influences of these parameters are necessary.

The well-known Nadal's criterion (1896) of the wheel climb derailments uses the lateral-to-vertical force limit (L/V limit) of a single wheel [8] depending on the angle of inclination of the wheel flange and friction coefficient. However, the latter changes in the wide range and laws of this variation are not sufficiently studied. Besides, the wheel climb derailments generally occur in situations where the climbing wheel experiences a high lateral force at great angle of attack, which is not considered in Nadal's formula. The number of experimental researches confirms the insufficient reliability of Nadal's criterion [14–16].

In **Figure 1** is shown a rail with a trace left on it after the wheel climbing [17]. The trace starts on the rail lateral surface and then passes on the rail tread surface.

The mechanism of generation and development of this trace is not studied sufficiently yet and needs additional researches [18]. Besides, according to this paper, friction coefficient in the contact zone of the wheel and rail reaches 0.5 and more at derailments.

The wheel climbing on the rail is also promoted by decreasing the rail radius of curvature and deviation of the axle of symmetry of the wheelset from radial position (increased angle of attack) that causes advancement of the wheel flange and railhead lateral surface contact point.

As it is known, a vertical axis of symmetry of the rail is inclined by 20° according to the standard. Deflection of the rail in the opposite direction that decreases the angle of inclination of the wheel flange is especially dangerous for the wheel climbing on the rail.

A creep is typical for the wheel and rail interaction. Different parts of interacting surfaces of the wheels and rails need to have different properties. Friction factor for the wheel flange and rail gauge face should be as low as possible—less than 0.1. Excessively high friction of the tread surfaces causes severe wear, plastic flow, and fatigue, and low friction can cause poor traction and braking. For tread surfaces of the wheel and rail, friction factor should not be less than 0.25 and greater than 0.4. Optimal value of the friction factor for these surfaces is 0.35 [12].

At common operational conditions, interacting surfaces are covered by various types of boundary layers—products of interaction of the surfaces and the environment, friction modifiers, etc.—that prevent a direct contact of the rubbing surfaces. Depending on the friction conditions, properties of the environment and surfaces, these layers may have various tribological properties that will have a great influence on the boundary friction [19–23]. This is confirmed by the results of the experimental researches in the inert gas environment and vacuum that excludes the possibility of interaction with the environment [2]. Under such conditions, unhindered seizure and intensive wear rate are observed.

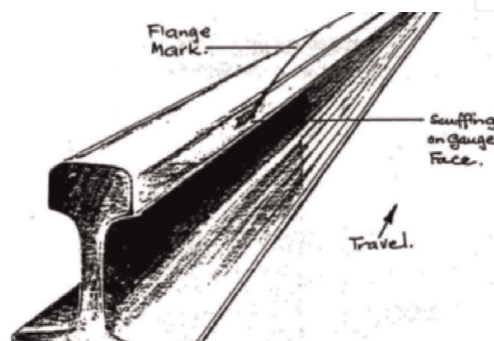


Figure 1.
The trace of the wheel climbing on the rail.

To prevent the aforementioned undesirable phenomena, it is important to provide the third body with due properties in the contact zone, control of the friction factor, and protection of the third body from destruction. However, until recently, despite considerable quantity of works, devoted to the study of dependences between wheel/rail and wheel/brake shoe friction forces and their durability, expected results are not obtained yet.

Our attention in the paper is mainly focused on the parameters that promote destruction of the third body. Some geometric features of the wheel and rail interaction and their influence on the friction path (sliding distance) and relative sliding velocity are shown. A corrected criterion of the wheel derailment is developed.

2. Dependence of the friction coefficient on the degree of destruction of the third body

The phenomenon of seizure is typical for interacting surfaces. This may occur when the third body is destroyed and the surfaces are juvenile (free from dirty, oxide films and adsorbed layers) and are approached sufficiently. Seizure of the interacting surfaces leads to the most dangerous and dominating kind of deterioration—scuffing.

For prevention of this phenomenon, they try to improve the tribological characteristics of the contact zone (improve properties of contacting surfaces and their ambient by applying the friction modifiers), stabilize the boundary layers, minimize a sliding distance and relative sliding velocity, etc. As it is noted in [23], the variation of the friction coefficient is mainly caused by changing a composition of the interfacial layer (the “third body”) between interacting surfaces. Our experimental researches have shown that for the given friction modifier, the variation of the friction coefficient mainly depends on the degree of destruction of the third body. An increase of the relative sliding velocity leads to an increase of the friction power and the contact temperature and decrease of the lubricant viscosity, film thickness, and friction force (friction coefficient). It corresponds to the “negative friction” in **Figure 2**, where a friction/creep relationship is shown [24].

Worsening of the working conditions is caused by the partial, unit seizures and nonprogressive damage of the third body in the separate unit places (**Figure 3**) that corresponds to the separate small impulses of the friction moment. In **Figure 3** are shown the stages of damage of the interacting surfaces due to seizures and scuffing of the surfaces.

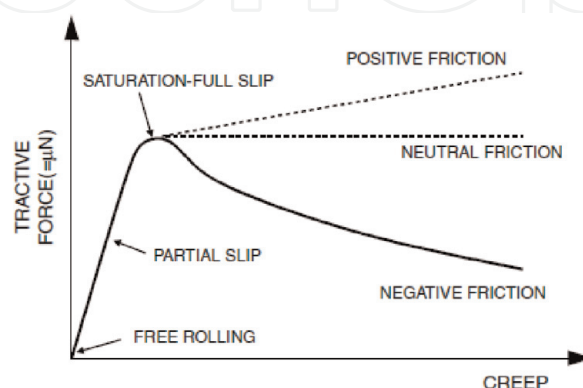


Figure 2.
 Friction/creep relationship.

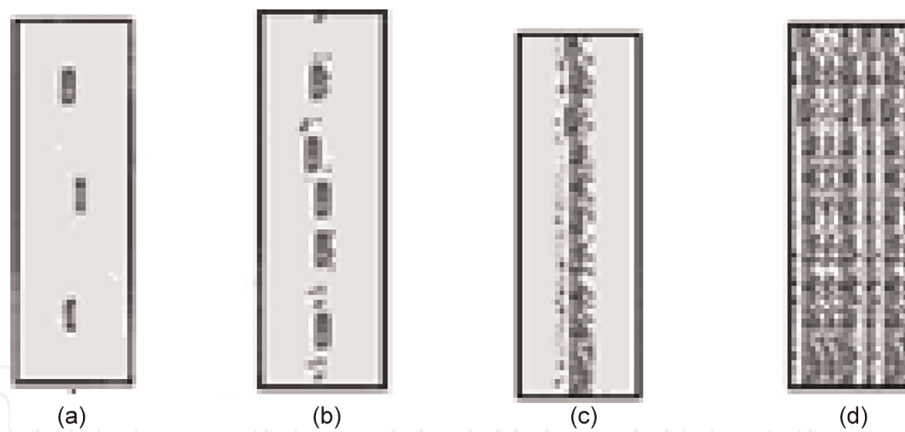


Figure 3. The stages of damage of the interacting surfaces due to seizures and scuffing of the surfaces: (a) unit seizures, (b) multiple seizures, (c) seizures in the form of the narrow strip, and (d) seizures on the whole area of the roller.

The further extension of destruction of the third body in the multiple places leads to the multiple damage of the third body, multiple adhesive junctions of micro-asperities, disruption of these junctions, and comparatively increased impulses of the friction moment and to “neutral friction.”

A progression of the third body destruction leads to spacious, discontinuous third body, adhesive junctions of micro-asperities, disruption of these junctions, and increase of the friction forces (“positive friction”). As it is seen from **Figure 2**, negative, neutral, and positive behaviors of the friction forces are stipulated by the degree of destruction of the third (**Figure 3**) body (the unit, multiple, narrow strip, and whole area).

Therefore, for ensuring the high wear resistance and stable friction force in the contact zone of the wheels and rails, it is necessary to provide continuous film of the third body with due properties between interacting surfaces. Consequently, a condition of destruction of the third body can be used as basics for estimation of the friction coefficient and the damages for the given peculiarities of the surface materials.

The various dominant damage types, wear rate, and friction coefficient are characteristic for various relative sliding. In **Figure 4** is shown dependence of the friction coefficient on the relative sliding and expected kind of surface damage. Three zones can be distinguished in **Figure 4**. In zone 1 and at the beginning of zone 2, deformations of the subsurface layers reach the maximum values, and the interacting surfaces undergo cyclic deformations. With the rise of relative sliding, the contact temperature gradually increases, decreasing viscosity of the third body [24] and the friction factor that reaches the minimum value. At full separation of the interacting surfaces by the third body, the tribo-technical properties of the contact zone mainly depend on the properties of the third body, and they provide high wear resistance of the interacting surfaces and relatively stable friction coefficient.

In zone 2 the separate small impulses of the friction moment and adhesive wear of low intensity correspond to destruction of the third body in the separate unit and multiple places, and balance between destruction and restoration of the third body is observed that stipulates the “mild” and “sever” wear [25]. In zone 3 destruction of the third body takes place in the narrow strips that passes then into whole area of interacting surfaces, resulting in rise of the friction coefficient, its instability, wear rate (reaching “catastrophic” wear), and scuffing.

So, we have three stages of variation of the friction coefficient and wear: at continuous third body, at reversible discontinuous third body, and at irreversible

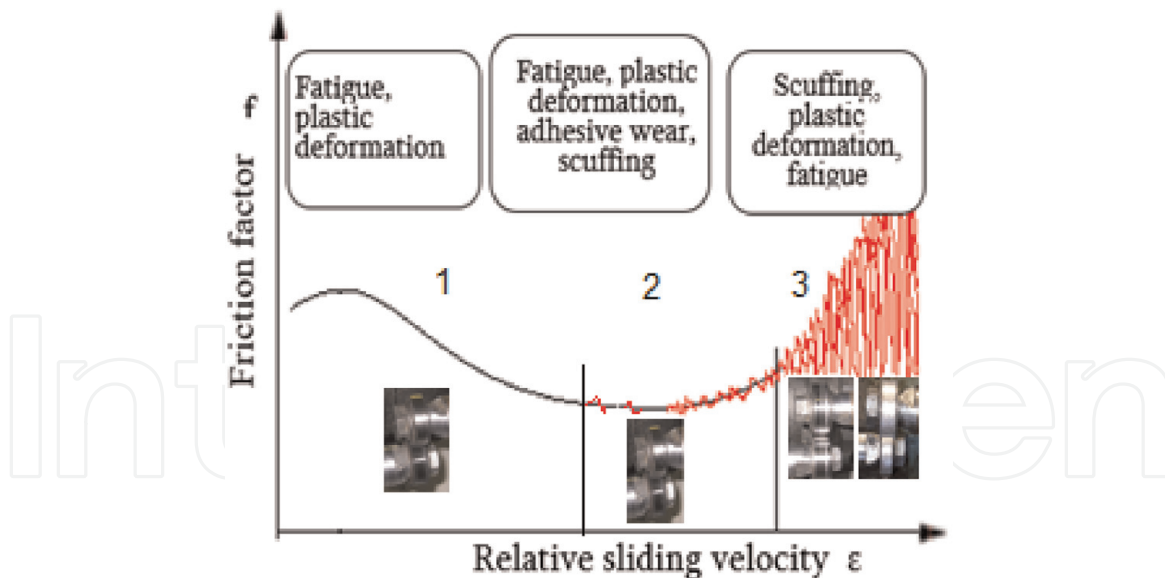


Figure 4.
 Dependence of the coefficient of friction (f) on the relative sliding (ϵ) and expected kind of surface damage.

discontinuous third body. The first stage is characterized by the minimal wear rate and stable friction factor. The second stage is characterized by the small constant and variable components of the friction coefficient. In terms of tribological characteristics, stages 1 and 2 indicate the acceptable working conditions of the tribological system. In contrast to this, stage 3 is characterized by the sharp increase of the constant and variable components of the friction coefficient, wear rate (“catastrophic wear”), vibrations, and noise, and operation in this zone is not admissible.

The friction coefficient is minimum and stable in the first and second zones, and its value depends mainly on the rheological properties of the third body. In the third zone, the friction coefficient is sharply increased and instable, and its value depends on the working conditions and properties of the surfaces, friction modifiers, and environment. The signs of the beginning of the third body are instability of the friction (coefficient) moment, vibrations, and noise, and at visual observation in the laboratory conditions, the signs of scuffing are noticeable. Its prediction is possible with the use of the tables and graphs considering the given friction modifier, working conditions and environment properties, as well as the criterion of destruction of the third body [26].

3. Some geometrical peculiarities of the wheel and rail interaction

The geometrical features of the wheel and rail interaction are stipulated by the designs of the rail track/bogie, wheel/rail, and their technical state. At lateral displacement of the wheelset relative to the rail, a contact point from the tread surfaces passes on the wheel flange root and rail corner, and the wheel and rail tread surfaces separate from each other. At further lateral displacement of the wheelset, the contact point passes on their steering surfaces, and the angle of inclination of the wheel flange increases up to 70° .

It is difficult to predict and control the friction forces, wear rate of various types, vibrations, and noise of the heavy loaded interacting surfaces of the railway transport running gear that decreases traffic safety, increases energy losses on friction, etc. Many works are devoted to the researches of dependences of the tribological

properties on various factors [1, 3–6], though their mechanisms of generation and variation are not always entirely clear that complicates the revelation of parameters influencing them [7, 8].

There are many reasons of generation of vibrations and noise at movement of the train, part of which are well studied and predictable, and ways of their decrease are known. The interacting surfaces of the wheels and rails are characterized by the various types of irregularities, 5–20 mm gaps in the rail joints, where the rail tread surfaces are spaced by 0.5–2 mm in the vertical direction; the various wear traces (rail corrugation, fatigue, etc.) and deviations from the wheel roundness are the sources of vibrations and noise.

The wheel and rail interaction is accompanied by the forced and self-excited vibrations of various frequencies, as the main reason of the forced vibrations is considered macro- and micro-asperities of the rail (periodic and separate asperities) [9–13]. However, the main source of the self-vibrations is friction between the wheel and rail. It must be noted that to various working conditions of the heavy loaded contacting surfaces and wear types correspond typical micro-asperities, which can be different from the initial micro-asperities [27, 28]. The researches have shown an important role of the tread and steering surfaces in generation of the vibrations (self-vibrations) and noise, whose reasons are not studied sufficiently. There is quite vague information on the reasons of the self-vibrations generated at interaction of the wheel and rail [9].

Generation of vibrations of the heavy loaded interacting elements of the railway transport running gear is stipulated by the complex processes proceeding in the contact zone. As a result of interaction of the surfaces with the environment, they are coated by the layers of various physical and chemical origins that are the components of the third body in the contact zone and have a great influence on the tribological properties of the contacting surfaces. According to observations by Godet, dry friction is largely determined not by the properties of materials of the contacting pair but by the characteristics of the structure and composition of the thin film that is formed on the surfaces of both bodies because of compaction of the wear product and its chemical composition and oxidation. Destination of the third body in the tribological systems is separation of the contacting surfaces, providing with the stable friction forces of proper values and protection of the surfaces against damage of various types. Tribological properties of the third body greatly depend on the initial properties of its component elements and features of the contact zone. The sliding velocity, power and thermal loading, and the sliding distance have especially great influence on the destruction of the third body. For providing the stability of the third body in the contact zone of the wheels and rails and reduction of the derailment probability, energy consumed on traction, environment pollution, and maintenance expenses, the decrease of the sliding distance and relative sliding is especially important.

The wheel/rail squeal in curves is the most common type of vibrations and noise. It is especially typical for high-speed movements, when because of various reasons, the relative sliding and sliding distance increase. This contributes destruction of the third body, seizure of the surfaces at direct contact, subsequent destruction of the seized surfaces, and instability of the friction forces and relative movement of surfaces.

Many negative phenomena (wear, noise, vibrations) are generated because of the wheel sliding on the rail. For elimination of the wheel sliding in the curves, the wheel tread surface is given a conical form with the intention of making the outer wheel to roll on the greater diameter passing the greater distance than the inner wheel and rotate both wheels through the equal angles, maintaining this way radial position of the wheelset axle. However, this intention can be realized only for a

certain combination of such parameters, as radius of the rail track curvature, mass and speed of the rolling stock, friction coefficient between the wheel and rail, etc. Therefore, practically the outer wheel rolls on the less diameter than necessary, and in the case of the free wheelset (without bogie), it falls behind the inner wheel, inclining the wheelset axle from the radial position.

In the case of the non-free wheelset, the bogie makes the wheelset maintain a radial position, forcing the outer wheel to roll the greater distance not to fall behind the inner wheel. Thereat, the outer wheel rotates through the greater angle than the inner one, and the wheelset axle is twisted. The angle of twist of the wheelset can increase up to the value that is stipulated by the friction force between the wheel and rail. When this angle of twist reaches the limited value, the wheel slides on the rail due to action of the wheelset axle elastic moment tending to bring it back to the equilibrium position.

Similarly, the wheel will slide on the rail at rolling in the straight rail track of the wheelset with the wheels of different diameters or with one wheel having an elliptical form. The mechanisms of the wheel sliding on the rail for the three noted cases are considered and explained in the next paragraphs.

3.1 Movement of the wagon wheelset in the curve

At pure rolling of the free wheelset (without bogie) in the curved rail track with radius of curvature R of the internal rail, its axle will be inclined from radial position because both wheels will have passed equal distances l. However, in the wagon wheelset rolling with velocity V, the outer wheel is constraint to maintain the radial position and pass greater distance $l + \Delta l$, rotating relative to the inner wheel in the clockwise direction if it is seen from axial direction A (Figure 5). At that, the wheelset axle is twisted through angle φ equal to the ratio of the difference Δl of the outer and inner arcs to the radius $D/2$ of the wheel tread surface, supposing that both wheels are rolling on the tread surfaces of equal diameters:

$$\varphi = 2\Delta l/D \tag{1}$$

From the drawing $\alpha = l/R = (l + \Delta l)/(R + \Delta R) = \Delta l/\Delta R$,
from where

$$\Delta l = l\Delta R/R, \tag{2}$$

and therefore

$$\varphi = 2\, l\Delta R/DR. \tag{3}$$

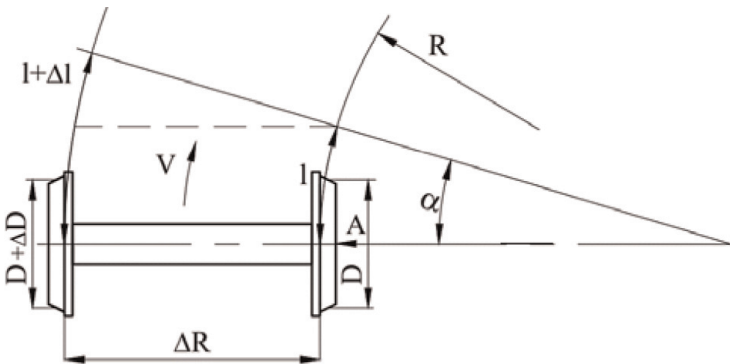


Figure 5.
Movement of the wagon wheelset in the curve and wheelset shaft slope from the radial position.

On the other hand, the maximum angle of twist of the wheelset axle φ_{\max} depends on the friction force

$$F = fQ \quad (4)$$

and is calculated by the known, from the resistance of materials, formula

$$\varphi_{\max} = ML/I_p G, \quad (5)$$

where M is a torque caused by the friction force

$$M = FD/2 = fQD/2; \quad (6)$$

f , friction coefficient; Q , vertical load (half of the load on the wheelset) of the wheel on the rail; L , length of the wheelset axle; I_p , polar moment of inertia of the wheelset axle cross section; and G , modulus of rigidity (shear modulus) of the axle material.

We determine distance between the worn-out segments of the rail or path l (at traveling this path, the wheels are rolling on the rail without sliding), at rolling of which the axle is twisted on the maximum angle φ_{\max} , from (3) replacing φ by φ_{\max}

$$l = DR \varphi_{\max} / 2\Delta R = MLDR / 2I_p G\Delta R \quad (7)$$

and putting the found l into (2) we obtain difference of the paths passed by the outer and inner wheels at which the axle is twisted on the maximum angle φ_{\max}

$$\Delta l = MLD / 2I_p G. \quad (8)$$

3.2. Movement of the wagon wheelset with the wheels of different diameters in the straight rail track

At rolling of the free wheelset (without bogie) with the wheels of different diameters D and $D + \Delta D$ in the straight rail track the distance l , the greater wheel passes a greater distance $l + \Delta l$, deflecting the wheelset axle from its perpendicular position relative to the rail track (**Figure 2a**). But in the wagon wheelset the axle being constraint to retain perpendicular position, the smaller wheel is forced to pass the same distance $l + \Delta l$ and rotate relative to the greater wheel in the clockwise direction, if it is seen from axial direction A . At that, the wheelset axle is twisted through angle φ that is determined by formula (1), from where, considering (5), we obtain the value of Δl (see formula (8)) corresponding to the maximum angle of twist φ_{\max} .

The following proportion can be written from the drawing: $(l + \Delta l)/l = (D + \Delta D)/D$ or $\Delta l/l = \Delta D/D$, from which we obtain distance l between the worn-out segments at passing of which the wheelset axle will be twisted through angle φ_{\max} :

$$l = \Delta l D / \Delta D = MLD^2 / 2I_p G\Delta D \quad (9)$$

3.3. Movement of the wagon wheelset with one elliptical wheel in the straight rail track

Consider a free wheelset with one wheel of diameter D and other elliptical wheel with the small D and bigger $D + \Delta D$ diameters moving in the straight rail track (**Figure 6a and b**).

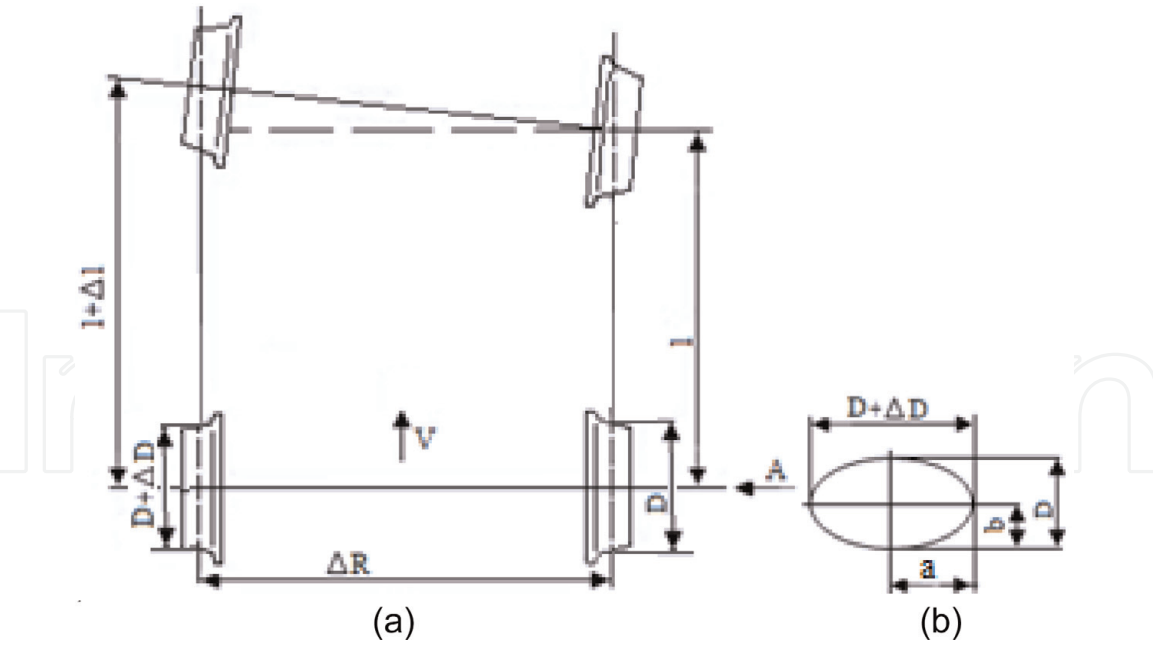


Figure 6.
Movement of the free wheelset in the straight rail track: (a) with the wheels of different diameters or with one elliptical wheel; (b) parameters of ellipticity.

At one revolution, these wheels will pass the different distances, correspondingly l and $l + \Delta l$, deflecting the wheelset axle from its perpendicular position relative to the rail track (**Figure 6a**). However, in the wagon wheelset the axle being constraint to retain perpendicular position, the wheel with diameter D is forced to pass the same (greater) distance $l + \Delta l$ and rotate relative to the elliptical wheel in the clockwise direction if it is seen from axial direction A . At that, the wheelset axle is twisted through angle φ that is determined by formula (1).

The difference of distances passed by the wheels at one revolution is $\Delta l = L - \pi D$, where the length of the elliptical tread surface

$$L = \pi[3(a + b) - (3a + b)(a + 3b)] \tag{10}$$

or

$$\Delta l = \pi[3(a + b) - (3a + b)(a + 3b)] - \pi D \tag{11}$$

The value Δl^I corresponding to maximum angle of twist φ_{\max} is obtained considering formula (5)

$$\Delta l^I = \varphi_{\max} D/2 = MLD/2I_p G \tag{12}$$

The distance l at passing of which the wheelset axle will be twisted on the angle φ_{\max} will be then

$$l = \pi D \Delta l^I / \Delta \tag{13}$$

In all the three cases considered above, at removing or decrease of the torque M acting on the wheel that takes place at its vertical vibrations when the friction force F decreases, the angle of twist of the axle will start to decrease. Suppose φ_{\max} falls down to zero during time t . This will take place at rotation of the inner wheel in the clockwise direction relative to the outer wheel on the angle φ_{\max} since the flange of the outer wheel is pressed on the rail and the friction force arisen between the flange and rail additionally restricts its movement. Obviously, during this time t the

inner wheel will roll and slide simultaneously on the rail and the rolling and sliding distance on the rail will be

$$S_r = Vt \quad (14)$$

We note that the rolling and sliding distance on the wheel tread surface is

$$S_w = \Delta l + S_r. \quad (14')$$

or for the variant of the elliptical wheel

$$S_w = \Delta l^I + S_r \quad (15)$$

here Δl or Δl^I is a sliding friction path and the wavelength of the worn-out rail (**Figure 3**)

$$W = l a s_{ers} \quad (16)$$

This value of the wavelength assumes that at release of the inner wheel, the friction force acting on it from the rail is zero. When the friction force differs from zero, the wavelength will be less since its both components will decrease and its value depends on the friction force magnitude.

To determine time t , we present the wheelset as a one-mass torsional vibratory system (**Figure 7a**), where C is a torsional rigidity of the wheelset axle and I , total moment of inertia of the inner wheel. Then, angle of twist φ_{max} will fall down to zero in conformity with a law of free vibrations of this vibratory system during the period $P/4$ (**Figure 7b**).

At that, period of free vibrations

$$P = 2\pi\sqrt{I/C} \quad (17)$$

and consequently, time t will be

$$t = P/4 = \frac{\pi}{2}\sqrt{I/C} \quad (18)$$

The average velocity of the wheel contact point relative to the wheel center (**Figure 8**)

$$V_w = -\frac{D\varphi_{max}}{2t} + V_r \quad (19)$$

where $V_r = -V$ is a velocity of the rail contact point relative to the wheel center.

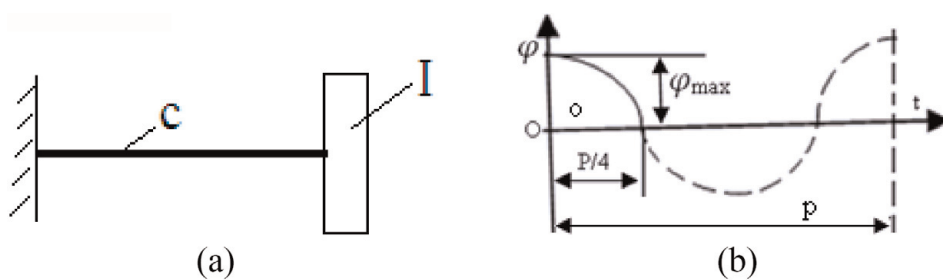


Figure 7.
(a) One-mass torsional vibratory system; (b) graph of the system free vibrations.

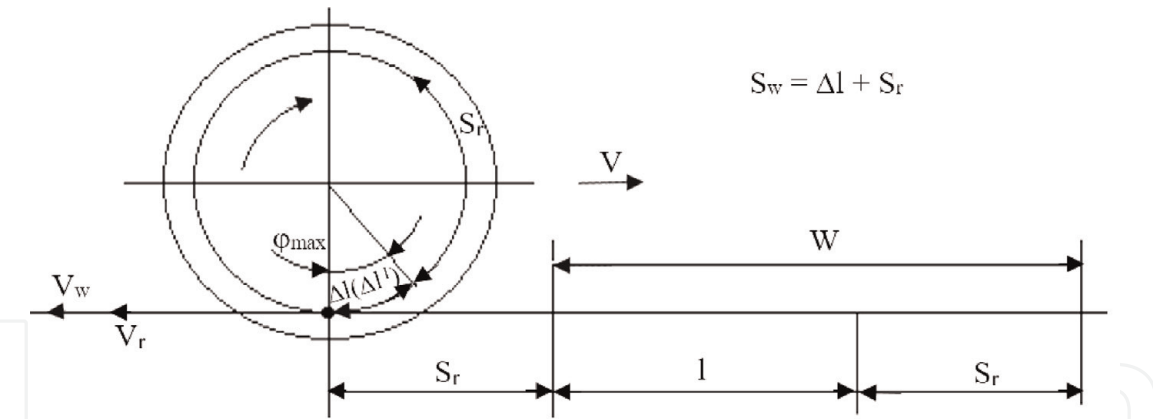


Figure 8.
The rolling and sliding distances on the rail and wheel.

We note that maximum velocity of the wheel contact point relative to the wheel center.

$$V_w^I = -\frac{A\omega D}{2} + V_r = -\varphi_{\max}\sqrt{\frac{C}{I}} \times \frac{D}{2} + V_r \quad (20)$$

where $A = \varphi_{\max}$ is an amplitude of the wheelset shaft torsion vibrations and $\omega = \sqrt{C/I}$ is cyclic frequency of vibrations.

Sliding velocity

$$V_{sl} = V_w - V_r \quad (21)$$

Relative sliding velocities

$$K_r = \frac{V_{sl}}{V_r} \times 100\% \text{ and } K_w = \frac{V_{sl}}{V_w} \times 100\% \quad (22)$$

The depth of the worn-out layer a year of the rail segment S_r .

$$h = i\Delta l N \quad (23)$$

where i is the wear intensity and N , number of cycles which is determined as follows:

$$N = N_1 N_2 N_3 N_4 \quad (24)$$

where N_1 is a number of the trains passing by a day; N_2 , number of wagons in the train; N_3 , number of wheels on one side of the wagon; and N_4 , number of days a year.

4. Conditions of derailment

Possibility of derailment or the wheel's rolling up on the rail is estimated by the criterion of the wheel flange contact point (point A, **Figure 9**) slipping down the rail lateral surface, based on the condition of equilibrium of forces acting on this point [24]. Lateral L and vertical V forces determined from the condition of equilibrium of these forces are. where N is a normal force; $F_f = fN$, friction force

between the wheel flange and rail lateral surface; f_l , friction coefficient between these surfaces; and β , angle of inclination of the wheel flange.

$$L = N \sin \beta - F_l \cos \beta \tag{25}$$

$$V = N \cos \beta + F_l \sin \beta \tag{26}$$

It should be noted that the forces acting on point A are interdependent and equalities (25) and (26) are only valid for limited values of forces L and V, since the rise of the friction force F_l is limited by the friction coefficient f_l . Therefore, at a certain ratio of forces L and V, the friction force F_l can no longer balance the contact point A, which will slip down on the rail lateral surface, and it is considered on this ground that the wheel cannot roll up on the rail. At that, equalities (25) and (26) become inequalities from where a criterion of impossibility of the wheel rolling up on the rail or derailment is obtained [24]:

$$\frac{L}{V} \leq \frac{\tan \beta - f^l}{1 + f^l \tan \beta} \tag{27}$$

However, at sign of equality (=) in (27) and to a certain extent at sign of inequality (<) also, the wheel can rotate about contact point A and roll up on the rail if such possibility exists or if moment of the force P acting on the wheel axle exceeds the moment of the vertical force V about contact point A (**Figure 10**). In other words, under such condition, two-point (O, A) contact of the wheel passes into one-point contact at A. In the first case (at sign =), the wheel will roll on the immobile point A with pure rolling, and in the second case (at sign <), the wheel will roll on the mobile point A creeping slowly down the rail lateral surface with combined rolling and sliding. Both cases lead to the wheel climbing the rail and derailment.

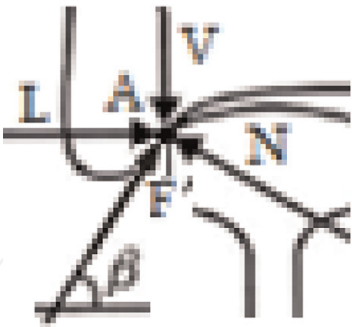


Figure 9.
Forces acting on the contact point a.

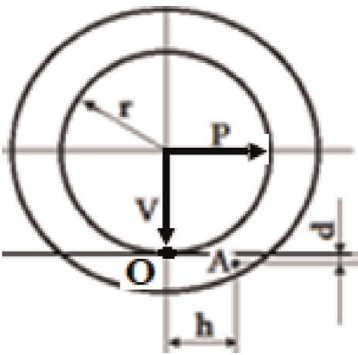


Figure 10.
Forces acting on the wheel axle.

Therefore, it is necessary to provide the criterion (27) with additional condition of impossibility of the wheel rolling on the contact point A, which, on the base of **Figure 10**, can be written as

$$Vh \geq P(r + d) \tag{28}$$

where h is the value of the climbing advance; r is the radius of the wheel rolling circle; d is the vertical coordinate of the contact point A.

Force P acting on the wheel axle cannot exceed the sum of the friction forces between the wheel and rail tread surfaces and between the wheel flange and rail lateral surface:

$$P \leq F + F_l = fV + f_l N \tag{29}$$

where f and f_l are friction coefficients between the wheel and rail tread surfaces and the wheel flange and rail lateral surfaces correspondingly.

Determining N and V correspondingly from (25) and (26), substituting them into (29) and then putting obtained P into (28), from the latter we obtain the following criterion of impossibility of the derailment:

$$\frac{L}{V} \leq \frac{h \left(\sin \beta - f^l \cos \beta \right)}{(r + d) \left(f \cos \beta + f f^l \sin \beta + f^l \right)} \tag{30}$$

If this criterion is not satisfied, the wheel starts to roll on the contact point A, and the contact between the wheel and rail tread surfaces is lost, or two-point contact at O and A passes into one-point contact at A. For obtaining a criterion of impossibility of the wheel rolling on the contact point A, it is necessary to put $f = 0$ in (30), which gives.

$$\frac{L}{V} \leq \frac{h \left(\sin \beta - f^l \cos \beta \right)}{(r + d) f^l} \tag{31}$$

The criteria (30) and (31) provide both, the wheel flange contact point sliding down the rail lateral surface and impossibility of the wheel rolling on this point. Besides, the criterion (30) ensures less value (more conservative) of the allowable ratio of the lateral and vertical forces L/V than criterion (27), while criterion (31), depending on the value of the climbing advance h , gives the ratio L/V less or more than criterion (27). For illustration, consider two variants of numerical data of the parameters:

- a. $\beta = 60^\circ$; $f = 0.4$; $f_l = 0.1$; $h = 62$ mm and $r + d = 485$ mm;
- b. $\beta = 60^\circ$; $f = 0.4$; $f_l = 0.1$; $h = 88$ mm and $r + d = 482$ mm.

Allowable maximum ratios L/V for these variants calculated by the criteria (27), (30), and (31) are given in the following table:

Variant	Criterion (27)	Criterion (30)	Criterion (31)
a	1.39	0.31	1.04
b	1.39	0.44	1.47

For analysis of the obtained results, suppose that ratio $L/V = 1.3$, i.e., criterion (27) is satisfied and derailment is not possible. However, it is seen from the table that for variant (a) neither criteria (30) nor (31) are satisfied and both predict derailment. For variant (b), criterion (30) is not satisfied, or it predicts derailment, and criterion (31) is satisfied, i.e., by this criterion, derailment is not possible. This means that the wheel starts to roll on the contact point A and two-point (O, A) contact passes into one-point contact at A. Then, this contact point slides down the rail lateral surface, the two-point contact restores, and so on, this process is repeated. However, at passing from two-point (O, A) contact into one-point contact at A, the lateral and vertical forces on the steering surfaces increase. Typical for these surfaces, increased relative sliding increases the power and thermal loads in the contact of these surfaces, generating the convenient conditions for destruction of the third body. This results in sharp increase of the cohesion forces, scuffing, and friction coefficient that promotes climbing of the wheel flange on the rail lateral surface. This is confirmed by the numerous laboratory researches carried out by us as well as the trace of the wheel climbing on the railhead lateral surface (**Figure 1**) that has a form of scuffing.

Thus, it is expedient to estimate possibility of derailment by criterion (30), since it provides both, the wheel flange contact point sliding down the rail lateral surface and impossibility of the wheel rolling on the same point, and ensures less value (more conservative) of the allowable ratio of the lateral and vertical forces L/V than criteria (31) and (27).

5. Conclusion remarks and future works

Prediction and avoiding of derailment are the most important problems of which many scientific works are devoted for their solution but the desirable results are not obtained yet. The survey of the literature and our experience show that the derailment is especially influenced by the friction coefficient that is not predictable, and in contrast to other parameters, it varies in a wide range.

It is shown that for prediction of the friction coefficient and providing its stability, it is necessary to provide the contact zone with the continuous and restorable third body of due properties.

The main results of the paper can be formed as follows:

- A friction factor as well as other tribological properties of interacting surfaces depends on the properties and degree of destruction of the third body.
- The sharp increase of the friction factor in the contact zone of steering surfaces indicates a beginning of the irreversible (progressive) destruction of the third body that contributes to the wheel climbing on the rail.
- For avoidance of derailment, decreasing the wear rate and ensuring sufficient durability of the rails, wheelsets, and brake shoes, a continuous or reversible third body must be provided in the contact zone.
- Destruction of the third body in the laboratory conditions is proposed to determine by the flash of the friction moment or criterion of destruction of the third body.
- A criterion of impossibility of derailment providing additionally impossibility of the wheel rolling on the wheel flange contact point is offered, which ensures

less value (more conservative) of the allowable ratio of lateral and vertical forces than Nadal's formula.

For solution of the problem of derailment, an experimental–theoretical approach is needed because of the lack of comprehensive theoretical model of the wheel climbing on the rail.

Due to the existence of materials with quite different designations and properties in the contact zone, many new unanswered problems rise. They are related with the further increase of the derailment criterion informativity and precision, providing the contact zone with the third body having due properties, conditions of formation, and destruction of the third body. They also concern to the tribological properties of the interacting metal and nonmetal surfaces, direct interaction of their juvenile surfaces and generation of the strong adhesion bonds, cold welding, destruction and wear of the surfaces, variation of the value, and instability of the friction coefficient.


On the base of experimental researches, we have ascertained dependence of the friction coefficient on the degree of destruction of the third body for the conditions of various relative sliding velocities, speeds, materials of interacting surfaces, roughness of the surfaces, friction modifiers, and loads at which the range of variation of the acting parameters is quite wide and therefore continuation of researches is needed.

Author details

George Tumanishvili*, Tengiz Nadiradze and Giorgi Tumanishvili
Institute of Machine Mechanics, Tbilisi, Georgia

*Address all correspondence to: ge.tumanishvili@gmail.com

IntechOpen

© 2019 The Author(s). Licensee IntechOpen. This chapter is distributed under the terms of the Creative Commons Attribution License (<http://creativecommons.org/licenses/by/3.0>), which permits unrestricted use, distribution, and reproduction in any medium, provided the original work is properly cited. 

References

- [1] Iijima H, Yoshida H, Suzuki K, Yasuda Y. Special edition paper. A Study on the Prevention of Wheel-Climb Derailment at Low Speed Ranges. JR EAST Technical Review-No. 30
- [2] Harris CL, Wyn-Roberts D. Friction and wear studies in ultra-high vacuum and the evaluation of electrical slip rings. In: Proceedings of the Institution of Mechanical Engineers, Conference Proceedings. Vol. 183; 1968. pp. 50-60
- [3] Huimin W, Nicholas W. Railway Vehicle Derailment and Prevention, Chapter 8 in Handbook of Railway Vehicle Dynamics, Edited by Simon Iwnicki. Taylor & Francis Group, LLC; 2006. pp. 209-239
- [4] Shust WC, Elkins JA, Kalay S, El-Sibaie M, Wheel-Climb Derailment Tests using AAR Track Loading Vehicle, Association of American Railroads Report R-910; 1997
- [5] Huimin W, Xinggao S, Nicholas W. Flange Climb Derailment Criteria and Wheel/Rail Profile Management and Maintenance Guidelines for Transit Operations. Transportation Technology Center, Inc. (TTCI). Washington, D.C: Pueblo, CO.; 2005
- [6] Weinstock H. Wheel Climb Derailment Criteria for Evaluation of Rail Vehicle Safety, Proceedings of ASME Winter Annual Meeting, 84-WA/RT-1. LA: New Orleans; 1984
- [7] Thompson DJ, Honk-Steel AD, Jones CJC, ISVR, Allen PD, Hsu SS, Iwnicki SD, MMU. Project A3 – Railway noise: curve squeal, roughness growth, friction and wear; 20th June, 2003
- [8] Wu H, Elkins J, Investigation of Wheel Flange Climb Derailment Criteria, Association of American Railroads Report R-931; July 1999
- [9] Cristol-Bulthe AL, Desplanques Y, Degallaix G. Coupling between friction physical mechanisms and transient thermal phenomena involved in pad-disc contact during railway braking. Laboratoire de Mrecanique de Lille (CNRS UMR 8107), Ecole Centrale de Lille, BP 48, F-59651 Villeneuve d'Ascq Cedex, France. Available online 23 May 2007
- [10] Elkins J, Wu H, New Criteria for Flange Climb Derailment, IEEE/ASME Joint Railroad. Conference, Newark, NJ, USA; April 4–6, 2000. pp. 1-7
- [11] Rhee SK, Jacko MG, Tsang PHS. The role of friction film in friction, wear and noise of automotive brakes. Wear. 1991; **146**(1):89-97
- [12] Vasic G, Franklin FJ, Kapoor A. Prepared for the Railway Safety and Standards board. University of Sheffield. Report: RRUK/A2/1; 2003
- [13] Weinstock H. Wheel climb derailment criteria for evaluation of rail vehicle safety. In: Proceedings of the ASME winter annual meeting; 1984. pp. 1–7
- [14] Iwnicki S. Handbook of Railway Vehicle Dynamics2. © 2006 by Taylor & Francis Group, LLC. p. 38
- [15] Braghin F, Bruni S, Diana G. Experimental and numerical investigation on the derailment of a railway wheelset with solid axle. Vehicle System Dynamics. 2006;**44**:305-325
- [16] Clementson J, Evans J. The use of dynamic simulation in the investigation of derailment incidents. Vehicle System Dynamics. 2002;**37**:338-349
- [17] Engineering Manual Track and Rolling Stock. TMC 213 Derailment

Investigation - Track and Rolling Stock.
Version 1.0; August 2011

and Delivery of Cargo on East-West
Routes, Springer. 2018. pp. 303-368

[18] Brian Marquis, Robert Greif.
Application of Nadal Limit in the
Prediction of Wheel Climb Derailment.
In: Proceedings of the ASME/ASCE/
IEEE 2011 Joint Rail Conference.
JRC2011. March 16–18, 2011. Pueblo,
Colorado, USA

[27] Elkins JA, Wu H. Angle of attack
and distance-based criteria for flange
climb derailment. *Vehicle System
Dynamics*. 1999;33:291-305

[19] Ahmed NS, Nassar AM. Lubrication
and lubricants. In: *Tribol. -Fundam.*
Adv. 2013. pp. 55-76

[28] Ishida H, Miyamoto T, Maebashi E,
Doi H, Iida K, Furukawa A. Safety
assessment for flange climb derailment
of trains running at low speeds on sharp
curves. *Quarterly Report of RTRI*
(Japan). 2006;47:65-71

[20] Yifei M, Turner KT, Szlufarska I.
Friction laws at the nanoscale. *Nature*.
2009;457:26. DOI: 10.1038/07748

[21] Hou K, Kalousek J, Magel E.
Rheological model of solid layer in
rolling contact. *Wear*. 1997;211:134-140

[22] Arthur A, Jannik T. Design of a Test
rig for Railway Curve Squealing Noise.
Sweden: Chalmers University of
Technology Gothenburg; 2017

[23] Drozdov YN, Pavlov VG,
Puchkov VN. Friction and Wear in the
Extreme Conditions (in Russian).
Mashinostroenie: Moscow; 1986. p. 224

[24] Eadie DT, Kalousek J, Chiddik KC.
The role of high positive friction (HPF)
modifier in the control of short pitch
corrugations and related phenomena.
Wear. 2002;253:185-192

[25] Lewis R, Dwyer-Joyce RS. Wear
mechanisms and transitions in railway
wheel steels. *Proceedings of the
institution of mechanical engineers, part
J. Journal of Engineering Tribology*.
2004;218(6):467-478

[26] Tumanishvili G, Natriashvili T,
Nadiradze T. Perfection of technical
characteristics of the railway transport
system Europe-Caucasus-Asia
(TRACECA) in the book. In:
Sladkowski A, editor. *Transport Systems*